Chain Dynamics: Diffusion and Viscoelastic Properties

System of small molecules

Langevin equation for Brownian motion $\xi \frac{dx(t)}{dt} = f(t)$ ξ is a friction, f(t) is a random force.

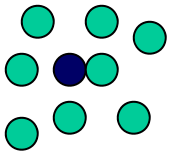

Diffusion

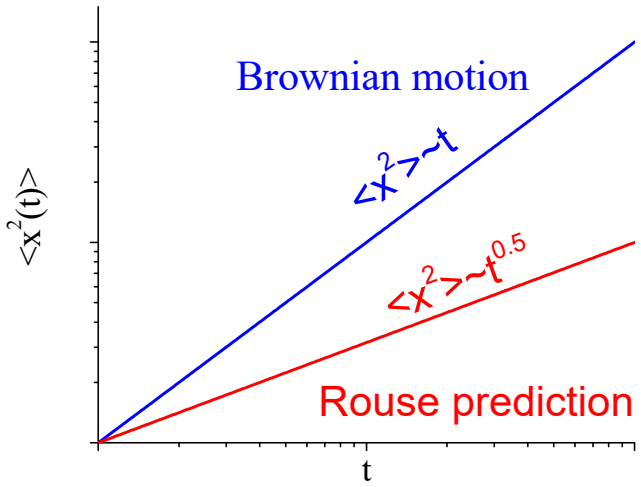

Loss modulus

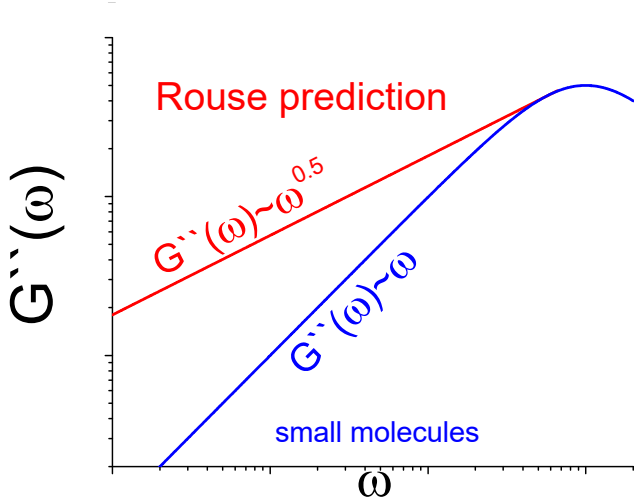

Polymeric system

Additional force appears in a polymer due to chain connectivity.

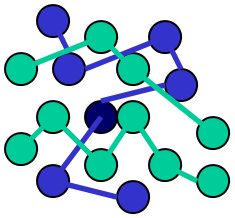

Rouse model assumes Gaussian statistics of the chain and:

It predicts: $\langle x^2 \rangle \sim t^{0.5}$ and $G``(\omega) \sim \omega^{0.5}$

$$\xi \frac{dx(t,n)}{dt} = \frac{3T}{a^2} \frac{\partial^2 x(t,n)}{\partial^2 n} + f(t)$$

Rouse model: *A Phantom Chain in a Solution*

For a long polymer chain one can move to continuous limit:

$$x_{n+1} - 2x_n + x_{n+1} \to \frac{\partial^2 x}{\partial^2 n} \Rightarrow\Rightarrow \xi \frac{\partial x(t,n)}{\partial t} = \frac{3T}{a^2}\frac{\partial^2 x(t,n)}{\partial^2 n} + f^r(t,n) \qquad (2)$$

This is a well-known diffusion equation.

We seek the solution of eq.(2) with the boundary conditions in the form:

$$x(t,n) = y_o(t) + 2\sum_{p=1}^{\infty} y_p(t)\cos\frac{\pi p n}{N}\text{; p=0,1,2,…, } y_o(t) \text{ is a position of the center of mass} \qquad (3)$$

Using Fourier transform: $y_p(t) = \frac{1}{N}\int_0^N dn \cos\frac{\pi p n}{N} x(t,n)$, these are *relaxation or Rouse modes*. Using that and eq.(2) for modes with p≠0:

$$\xi\frac{\partial y_p(t)}{\partial t} = -\frac{\xi}{\tau_p} y_p(t) + f_p(t)\text{; here } \tau_p = \frac{N^2 a^2 \xi}{3\pi^2 T p^2}; f_p(t) = \frac{1}{N}\int_0^N dn f^r(t,n)\cos\frac{\pi p n}{N} \qquad (4)$$

and for p=0 $\qquad \xi\frac{\partial y_0(t)}{\partial t} = f_0(t)$

Hence forces $f_p(t)$ are independent of one another the Rouse equation (2) decomposes into a set of independent equations (4). Thus, motion of polymer chain can be represented as a superposition of independent Rouse modes.

Examples

1. Let's consider end-to-end vector relaxation: $R(t) = x(t,N) - x(t,0) = -4 \sum_{p=1,3,5,\ldots} y_p(t)$

$$\langle R(t)R(0)\rangle = 16 \sum_{p=1,3,5,\ldots} \langle y_p(t) y_p(0)\rangle = \frac{8Na^2}{\pi^2} \sum_{p=1,3,5,\ldots} \frac{1}{p^2} \exp(-\frac{t}{\tau_p}) \qquad (5)$$

here $\tau_p = \frac{\tau_1}{p^2}; \tau_1 = \frac{N^2 a^2 \xi}{3\pi^2 T}$ *important* $\tau \propto N^2$ (6)

The modes with small p decay most slowly, especially p=1. The mode with p=1 defines the behavior of the correlation function, eq.(5), at long t. The amplitude of this mode is largest. Due to that reason in many approximations only mode with p=1 is considered.

Modes with p>1 can be regarded as the maximum relaxation time for a chain section *N/p* links, e.g. motion on length scales $\sim a(N/p)^{1/2}$.

2. Diffusive motion of the coil as a whole. Because $y_o(t)$ represents the center of mass motion, mean-squared displacement of the coil:

$$\langle [y_0(t) - y_0(0)]^2 \rangle = 6 \frac{T}{N\xi} t = 6 D_{coil} t; \qquad \textit{important} \quad D_{coil} = \frac{T}{N\xi} \qquad (7)$$

It corresponds to additive friction forces acting on every individual monomer link.

3. Displacement of a link with time. From eq.(2), taking into account $\langle y_p(t) y_q(t') \rangle = 0$ for p≠q:

$$\left\langle [x(t,n) - x(0,n)]^2 \right\rangle = \left\langle [y_0(t) - y_0(0)]^2 \right\rangle + 4 \sum_{p=1}^{\infty} \cos^2 \frac{\pi p n}{N} \left\langle [y_p(t) - y_p(0)]^2 \right\rangle =$$

$$= \frac{6T}{N\xi} t + \frac{4Na^2}{\pi^2} \sum_{p=1}^{\infty} \frac{1}{p^2} \cos^2 \frac{\pi p n}{N} \left[1 - \exp(-\frac{t}{\tau_p}) \right] \qquad (8)$$

For long times, $t >> \tau_1$, the second term is negligible. Thus the displacement of the link follows the center of mass of the coil.

At short times, $t << \tau_1$, for a link far from the chain end:

$$\left\langle [x(t,n) - x(0,n)]^2 \right\rangle \approx \frac{4Na^2}{\pi^2} \int_0^{\infty} \frac{dp}{2p^2} \left[1 - \exp(-\frac{tp^2}{\tau_1}) \right] = \left(\frac{12Ta^2}{\pi\xi} t \right)^{1/2} \qquad (9)$$

a) As it is expected for short times, there is no dependence on N.

b) The displacement increases much slower with time $\sim t^{1/4}$ in comparison with a free Brownian motion. Thus connectivity slows down the diffusive motion of a segment.

Experiments in dilute Θ-solution: $\tau \propto N^{3/2}$; $D_{coil} \propto N^{-1/2}$

This behavior corresponds to a rotational time and diffusion of a sphere with the radius $R \sim aN^{1/2}$.

Zimm Model: A Phantom Chain with Hydrodynamic Interaction

Schematic presentation of the flow field

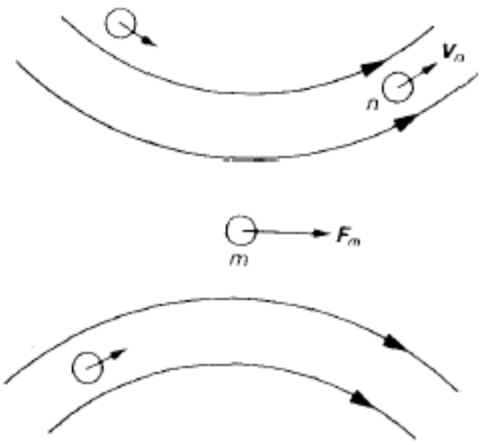

The motion of the solvent, entrained by the polymer link, influences the motion of other links. This is a long range interaction which couples the motion of different segments strongly.

$$6\pi\eta_s \frac{\partial x(n,t)}{\partial t} = \int_0^N dm \left\langle \frac{1}{|r_{n-m}|} \right\rangle \left[\frac{3T}{a^2} \frac{\partial^2 x(m,t)}{\partial^2 m} + f^r(m,t) \right]$$

Important difference with the Rouse picture is that the Rouse modes $y_p(t)$ are coupled now.

$$\frac{\partial y_p}{\partial t} = -\frac{1}{\tau_p} y_p(t) + \frac{1}{\sqrt{3\pi^3 p}} \frac{N^{1/2}}{a\eta_s} f_p(t); \tau_p = \sqrt{\frac{3}{\pi}} \frac{N^{3/2} a^3 \eta_s}{T p^{3/2}}$$

Thus $\tau_1 \sim N^{3/2}$ also in agreement with experimental data.

It is interesting to note that $\tau_1 \propto \frac{\eta_s N^{3/2} a^3}{T} \propto \frac{\eta_s R_D^3}{T}$ corresponds to the characteristic time of rotational relaxation of solid sphere of radius R_D.

Thus the hydrodynamic interactions lead to a non-draining of polymer coil. It behaves like a sphere of radius R_D.

Neutron Scattering [B.Ewen, D.Richter, Adv.Pol.Sci. V.134, 1 (1997)]

Due to much shorter wavelength is more suitable for analysis of the range qRg>>1.

Θ-conditions

$\Gamma_q \propto q^4$ for the Rouse model and $\Gamma_q \propto q^3$ for the Zimm model.

Analysis demonstrates qualitative agreement with the predictions of the Zimm model.

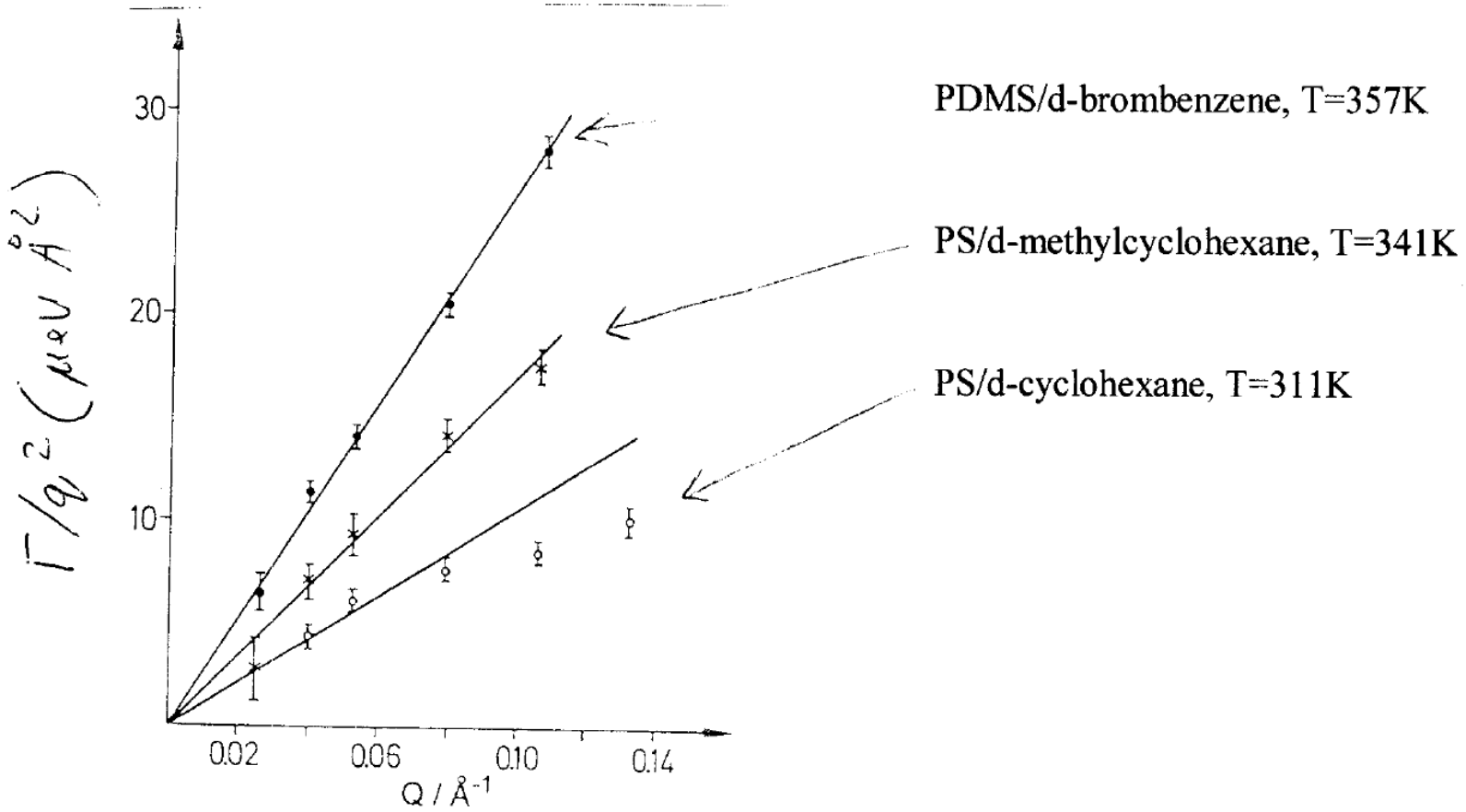

Dynamics in the melt and concentrated solutions

Tube model

The main model for the case of concentrated systems is a tube model. It considers the Brownian motion of a chain moving through a fixed network. The motion of the chain is almost confined in a tube-like region.

(a)

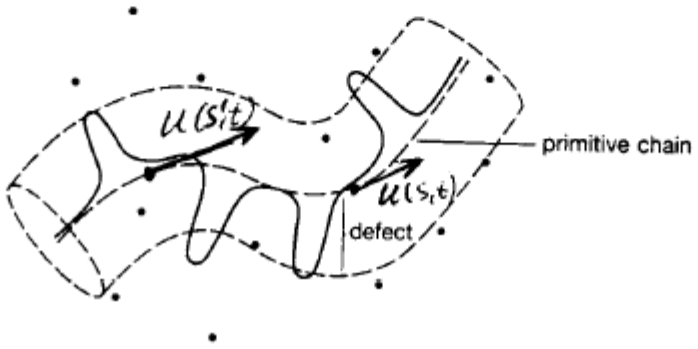

Reptation

In the short-time scale the motion of the polymer is regarded as wriggling around the primitive path.

On a longer time-scale the conformation of a primitive path changes. For large-scale motion one disregards the small-scale fluctuations and considers the *primitive chain*.

Assumptions for the dynamics of primitive chain:

1. The primitive chain has constant contour length L.
2. The primitive chain can move back and forth only along itself with certain D_t.
3. The correlation of the tangent vectors u(s,t) and u(s',t) decreases quickly with $|s-s'|$ (Gaussian-like behavior for the primitive chain).

Important parameter – N_e is an average number of segments between entanglements. The characteristic scale, $d \sim aN_e^{1/2}$, corresponds to effective tube diameter.

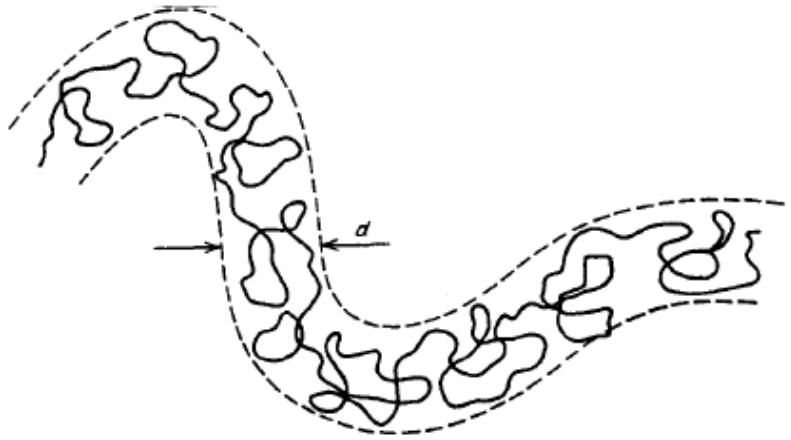

On length scales r<d the chain is insensitive to entanglements and performs a random walk around the primitive path.

On large scale (r>>d) *the primitive path is also Gaussian with an effective segment length d*. The total contour length: $L \sim d\frac{N}{N_e} \sim a\frac{N}{N_e^{1/2}}$.

Qualitative consideration

The hydrodynamic (and the excluded volume) interactions are screened at $r \sim \zeta \sim a$. Thus the interactions is totally screened and the friction term is a sum of the friction forces acting on each link: $\xi_t \sim N\xi \sim N\eta_s a$

The diffusion coefficient for reptation along the tube: $D_t = kT/\xi_t \sim \frac{kT}{N\eta_s a}$ (1)

The maximum relaxation time of the polymer melt or concentrated solution is achieved when the chain creeps out of the initial tube:

$$\tau^* \sim \frac{L}{D_t^2} \sim \frac{\eta_s a^3 N^3}{N_e kT} \quad (2)$$

The self-diffusion coefficient: $D_{self} \sim \frac{R^2}{\tau^*} \sim \frac{N_e kT}{N^2 \xi}$

Let's consider the mean square displacement of a point on the primitive path $\langle [x(s,t)-x(s,0)]^2 \rangle$. It diffuses with the diffusion coefficient D_t.

$$\left\langle [x(s,t)-x(s,0)]^2 \right\rangle = 2\frac{d}{L} D_t t + \sum_{p=1}^{\infty} \frac{4Ld}{\pi^2 p^2} \cos^2 \frac{\pi p s}{L} \left[1 - \exp(-\frac{p^2 t}{\tau^*}) \right] \qquad (4)$$

For $t >> \tau^*$ the first term dominates:

$$D_{self} = \lim_{t \to 0} \frac{\left\langle [x(s,t)-x(s,0)]^2 \right\rangle}{6t} = \frac{dD_t}{3L} = \frac{dL}{3\pi^2 \tau^*} \sim \frac{R^2}{\tau^*} \qquad (5)$$

Thus, there are 4 different regimes for $\langle \Delta x^2 \rangle$.

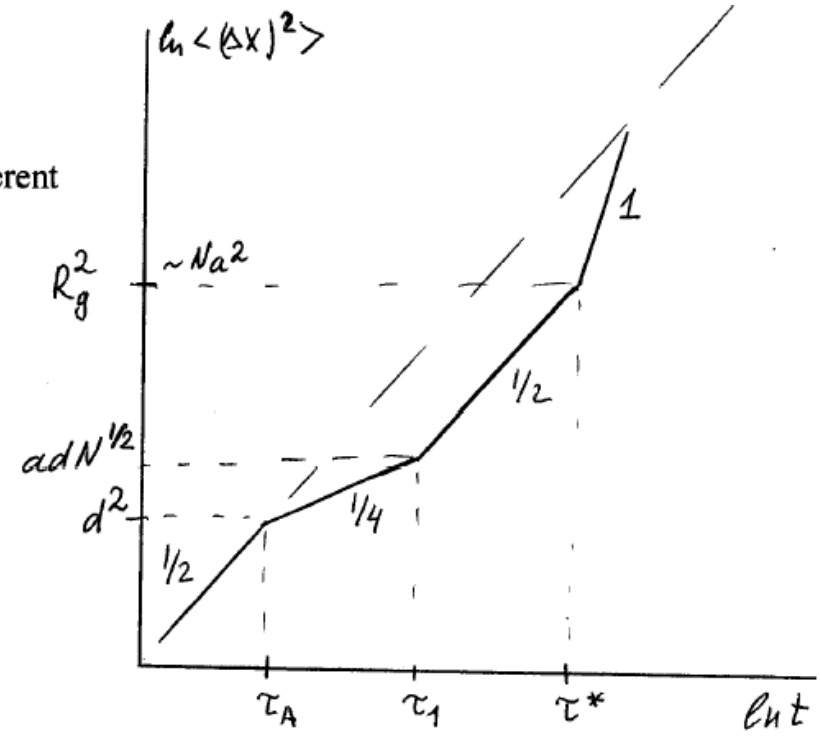

Data for cis-1,4-polyisoprene with different M_w [Dielectric Spectroscopy of Polymeric Materials, Ed. J.P.Runt, J.J.Fitzgerald, p.97-102]

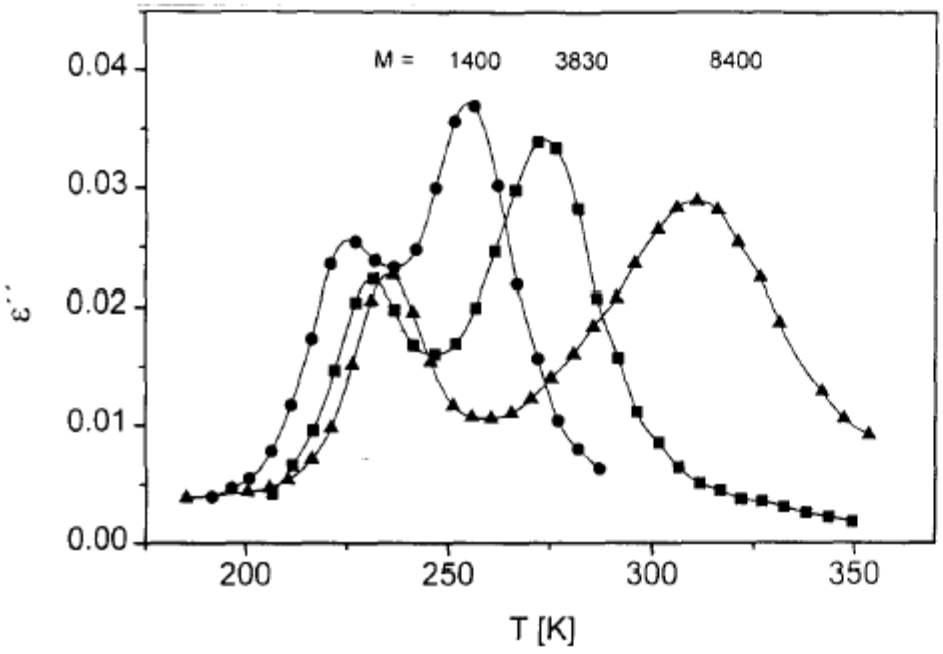

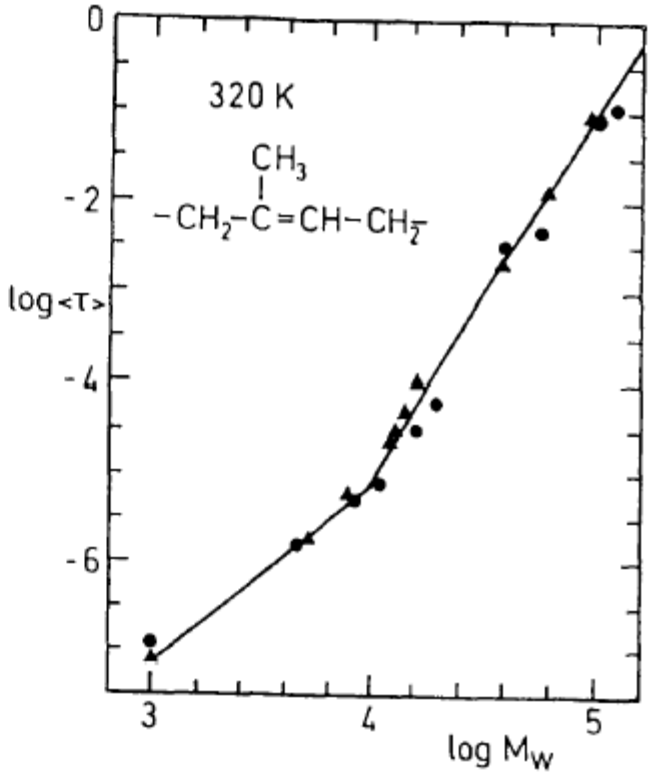

At low M_w the relaxation time $\tau \sim M^2$ (Rouse behavior), while at higher M_w $\tau \sim M^{3.7}$ is observed (the exponent is higher than expected from the reptation model).

Dependence of τ^* on N

$\tau^* \sim N^3$ does not agree with experiment: $\tau^* \sim N^{3.4}$.

The generally accepted explanation is associated with *fluctuations of the contour length L.*

Rouse model

The modulus: $$G(t) = \frac{c}{N} kT \sum_p \exp(-2tp^2/\tau_R); \tau_R = \frac{\xi N^2 a^2}{3\pi^2 kT} \quad \sim M^2$$

The viscosity: $$\eta_o = \int_0^\infty dt G(t) = \frac{c\xi}{36} N a^2 \quad \sim M$$

$$G(t) = G_N^0 \psi(t) = G_N^0 \sum_{p=1,3,\ldots} \frac{8}{p^2\pi^2} \exp\left(-\frac{p^2 t}{\tau^*}\right); \tau^* = \frac{\xi N^3 a^2}{\pi^2 kTN_e} \qquad (5)$$

G(t~ τ_A) should approach the value of G_N^0:

$$G_N^0 \sim G(\tau_A) \approx \frac{c}{N} kT \left(\frac{\tau_R}{\tau_A}\right)^{1/2} \approx \frac{ckT}{N_e}$$

That gives G(t) in the whole time range.

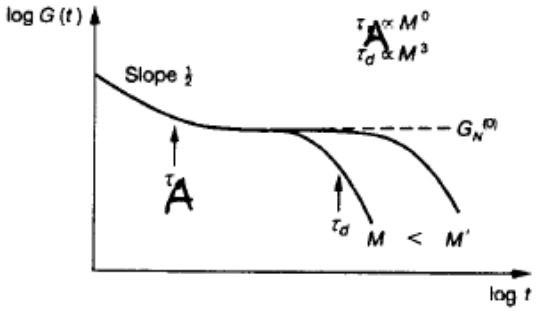

The complex modulus for $\omega\tau_A >> 1$:

$$G'(\omega) = G''(\omega) = G_N^0 \left(\frac{\pi\omega\tau_A}{2}\right)^{1/2}$$

and for $\omega\tau_A << 1$:

$$G'(\omega) = G_N^0 \sum_{p=1,3,\ldots} \frac{8}{\pi^2 p^2} \frac{\omega^2\tau^{*2}}{p^4 + \omega^2\tau^{*2}}$$

$$G''(\omega) = G_N^0 \sum_{p=1,3,\ldots} \frac{8}{\pi^2} \frac{\omega\tau^*}{p^4 + \omega^2\tau^{*2}}$$

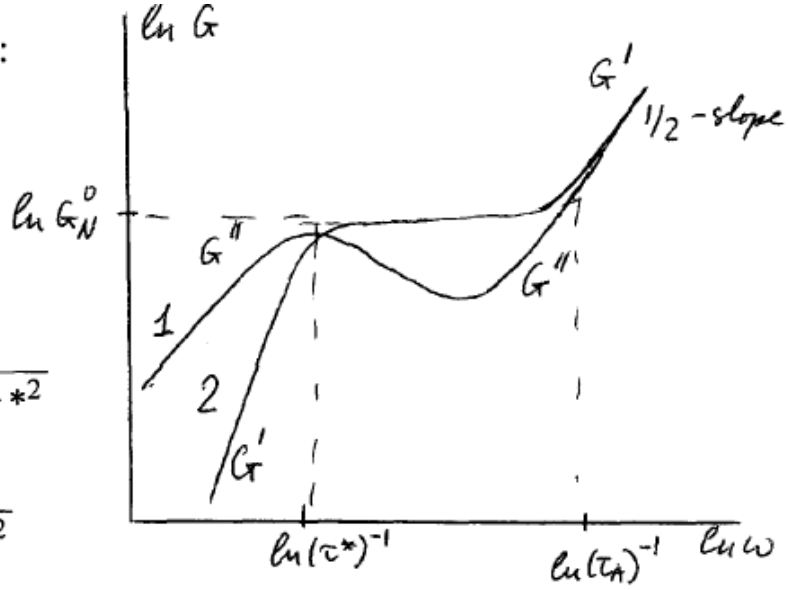

The viscosity and the steady-state compliance will be defined mostly by the integral at $t>\tau_A$:

$$\eta_0 \approx \int_{\sim\tau_A}^{\infty} dtG(t) \approx G_N^0 \int_0^{\infty} dt\psi(t) = \frac{\pi^2}{12} G_N^0 \tau^* \sim \frac{\xi c a^2 N^3}{N_e^2}$$

$$J_e^0 \approx \frac{1}{\eta_0^2} \int_{\sim\tau_A}^{\infty} dtG(t)t \approx \frac{1}{\eta_0} \int_0^{\infty} dt\psi(t)t \approx \frac{6}{5G_N^0} \sim \frac{N_e}{ckT}$$

Storage modulus for PS melts with different M_w

J_e^0 for PS at T=160C, dashed line shows the result of the Rouse model.

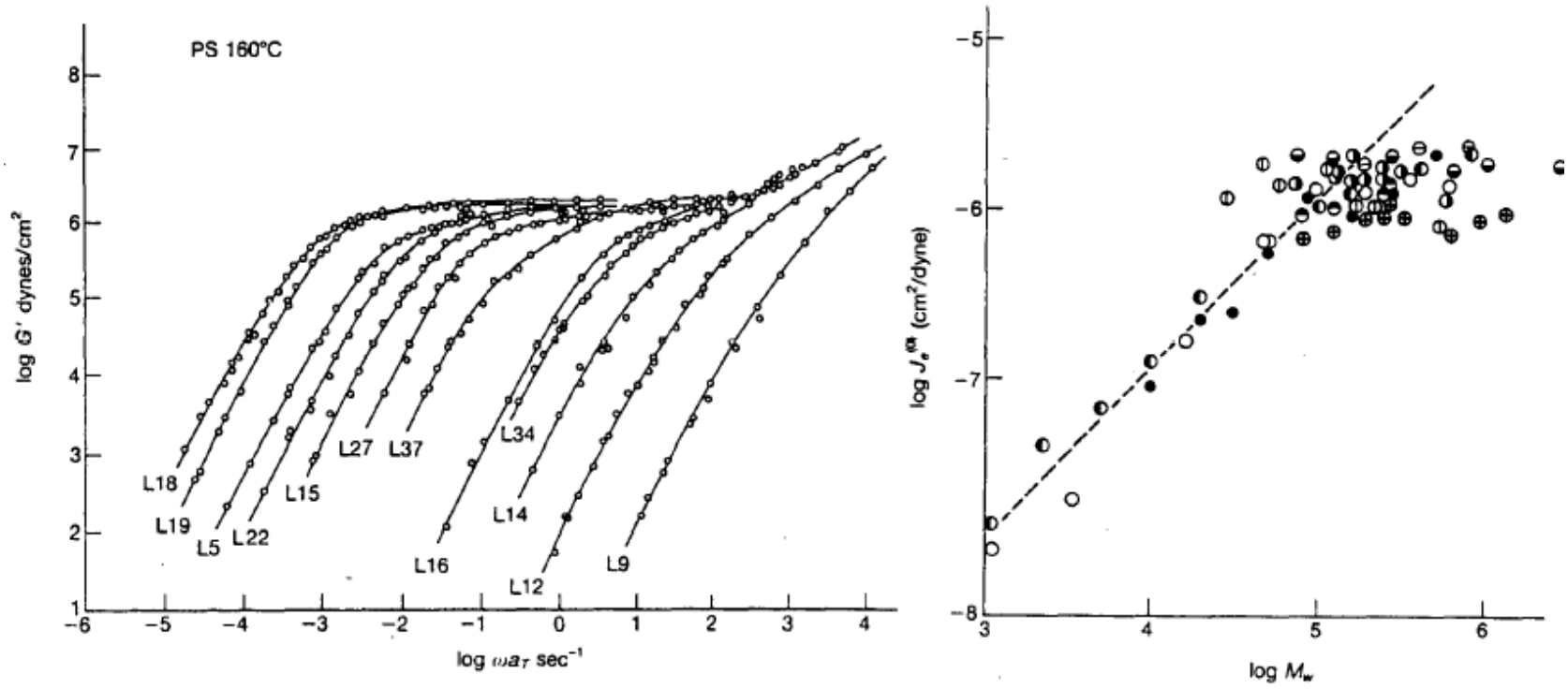

Steady-state viscosity of various polymers in melt

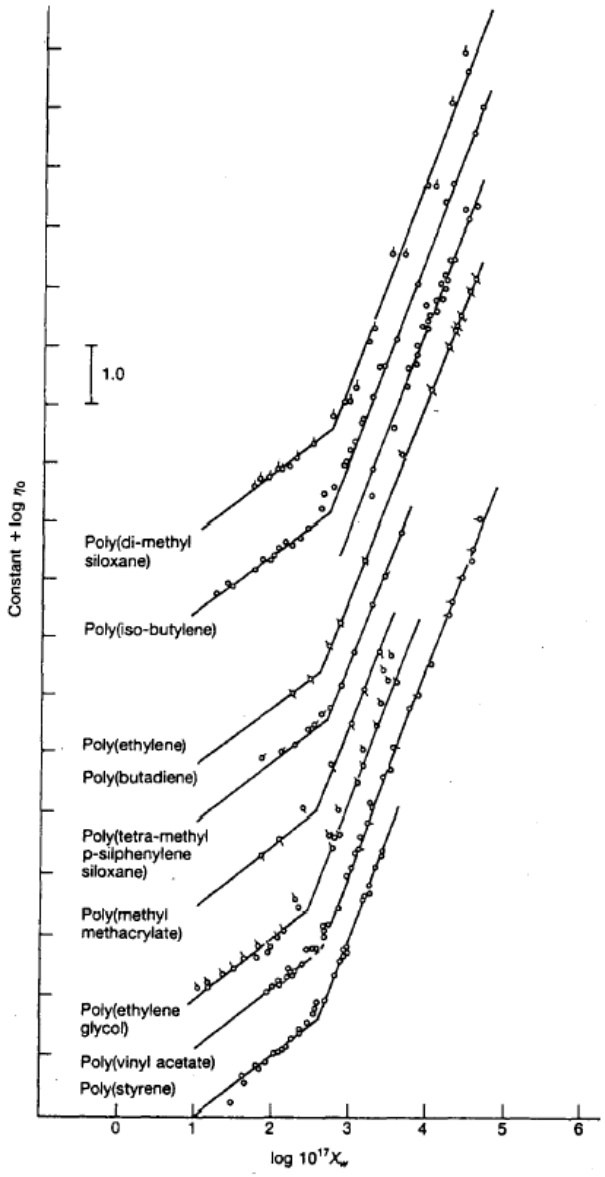

At low $M_w \sim X_w$ the Rouse behavior $\eta \sim M_w$ is observed.

At higher Mw the viscosity is increasing even faster than predicted by the reptation model: $\eta \sim M_w^{\mu}$, $\mu \sim 3.4$.

One of the explanations relates the disagreement to low M_w of polymers used for the measurements. It seems that the experimental value is reaching the theoretical prediction at extremely high $M_w \sim 800 M_c$.

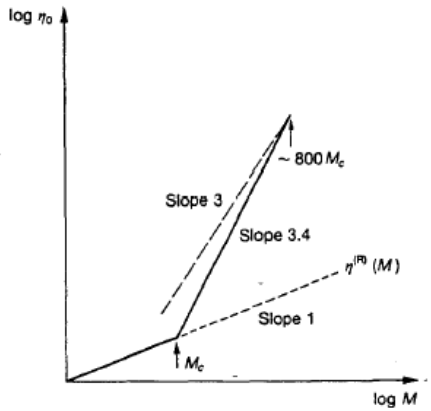

Rubber Elasticity

[*J.E.Mark, B.Erman, Rubberlike elasticity, a molecular primer*]

One of the most remarkable properties of polymers, which have no apparent counterpart in low-weight molecular systems, is elasticity. Rubber-like elasticity is a particular property of the network formed by long molecules joined at some cross-linking points.

Molecules must be long, highly flexible, should be chemically crosslinked. Cross-linked polymers can have very high elongation and still remain elastic (can return to its initial state).

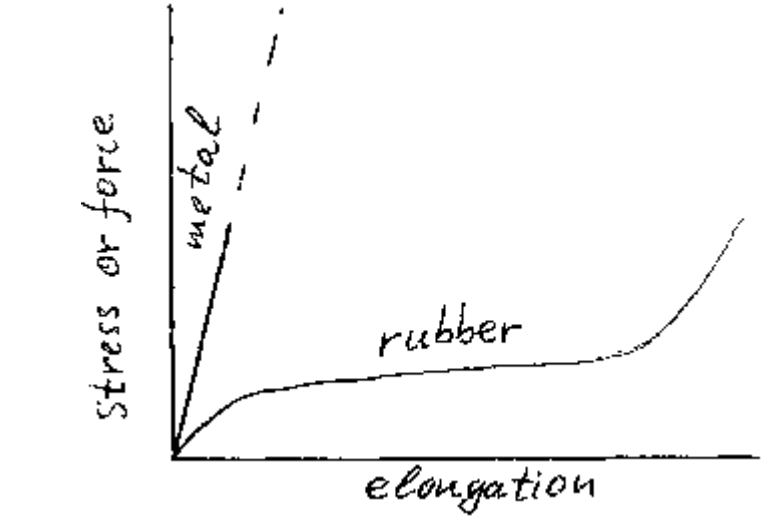

The molecular origin of the elastic force f can be elucidated through thermoelastic experiments.

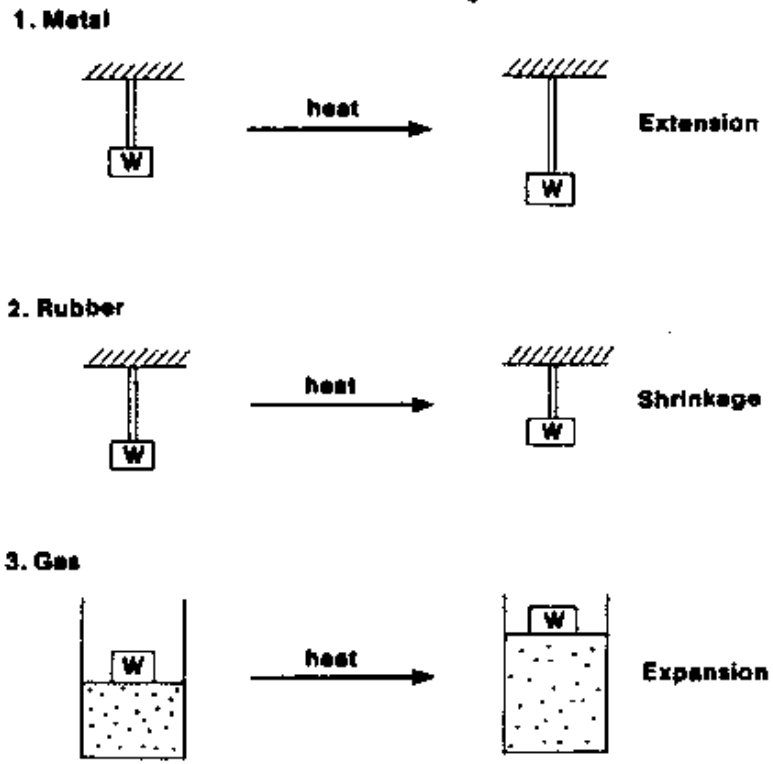

Different mechanisms of elasticity.

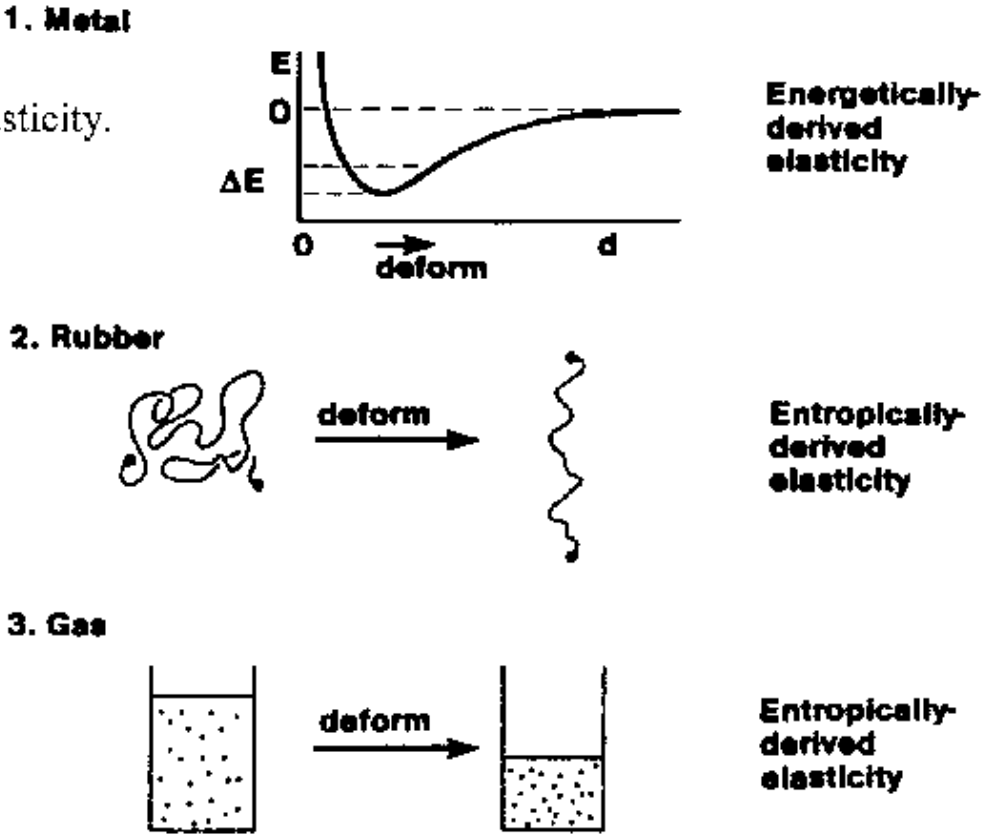

Rubber state is a specific state: Polymer may be above its melting temperature, i.e. in a liquid state, however, due to chemical crosslinks rubber keeps its shape as a solid matter.

Two basic postulates of molecular theories of rubber-like elasticity:

✓Rubber-like elasticity is an *intramolecular effect*, i.e. intermolecular interactions do not play significant role;

✓The Helmholtz free energy should be separable, $A=A_{liq}(T,V,P)+A_{el}(\lambda)$, ($\lambda$ is the strain tensor), i.e. *liquid-like part of the free energy is independent of deformation*.

Rubber-like polymers

Polymer	Structure	T_g (°C)	T_m (°C)
Natural rubber[a]	$[C(CH_3)=CH-CH_2-CH_2-]$	−73	28
Butyl rubber[b]	$[C(CH_3)_2-CH_2-]$	−73	5
Poly(dimethylsiloxane)	$[Si(CH_3)_2-O-]$	−127	−40
Poly(ethyl acrylate)[c]	$[CH(COOC_2H_5)-CH_2-]$	−24	—
Styrene–butadiene co-polymer	$[CH(C_6H_5)-CH_2-]$, $[CH=CH-CH_2-CH_2-]$	Low	—
Ethylene–propylene copolymer	$[CH_2-CH_2-]$, $[CH(CH_3)-CH_2-]$	Low	—

[a] *Cis*-1,4-polyisoprene.

[b] Polyisobutylene containing a few mole percent unsaturated comonomer.

[c] Stereochemically irregular (atactic) polymer.

The essential feature of rubber elastic system is a network, the *junction points* of which are connected by *long flexible randomly coiled polymer chains*. The detailed chemical nature of the atoms comprising the chains is not important.

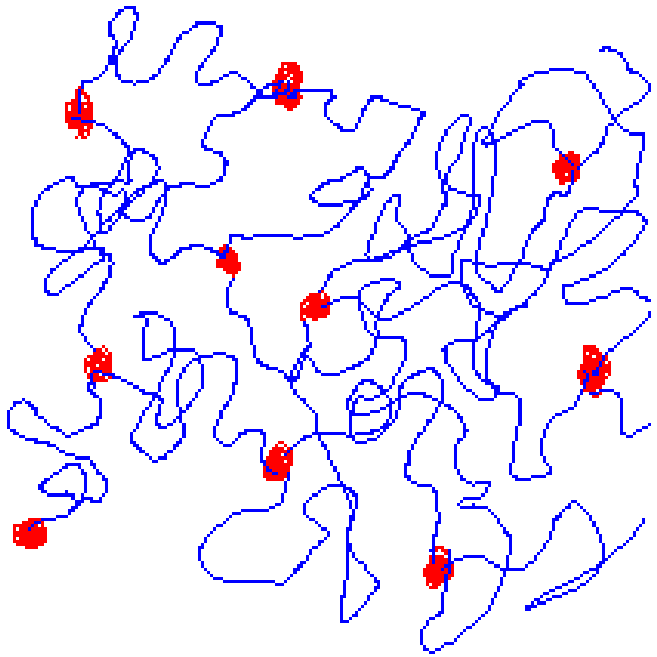

Structure of Networks

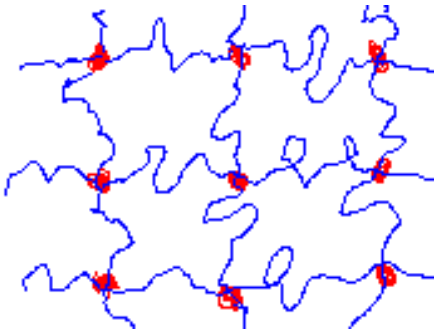

Network with ϕ=4

The number of chains meeting at each junction is called functionality ϕ. Another important parameters of the network:
- Mc – averaged molecular weight between junctions;
- ν – the number of network chains;
- μ – the number of junctions;
- ξ – the cycle rank (the number of chains that have to be cut in order to reduce the network to a tree with no closed cycles.

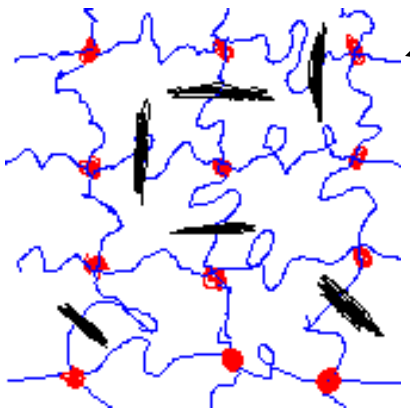

These 5 parameters are not independent. The number of chain ends, $2\nu=\phi\mu$.

The other relationships are not so obvious:

$\xi \approx \nu-\mu=\nu(1-2/\phi)$; $\xi/Vo=(1-2/\phi)\rho Na/Mc$

Here Vo is the volume of network in the state of formation, ρ is the corresponding density, Na is the Avogadro's number.

Elementary statistical theory for idealized networks

The elastic free energy of a single chain at fixed r can be written:

$$A_{el} = c(T) - TS = c(T) - kT \ln P_N(r) = c(T) + \frac{3kT}{2\langle r^2 \rangle_0} r^2$$

Then the force: $$f = \frac{\partial A_{el}}{\partial r} = \frac{3kT}{\langle r^2 \rangle_0} r \approx \frac{3kT}{Na^2} r$$

The total elastic free energy of the network relative to the undeformed state is obtained by summing over the ν chains of the network:

$$\Delta A_{el} = \frac{3kT}{2\langle r^2 \rangle_0} \sum_{\nu} \left[r^2 - \langle r^2 \rangle_0 \right] = \frac{3}{2} \nu kT \left[\frac{\langle r^2 \rangle}{\langle r^2 \rangle_0} - 1 \right] \qquad \textbf{(1)}$$

$\langle r^2 \rangle = \sum_{\nu} r^2 / \nu$ is the average mean-squared end-to-end chain vector in the deformed network.

So, we need to relate $\langle r^2 \rangle = \langle x^2 \rangle + \langle y^2 \rangle + \langle z^2 \rangle$

to the undeformed value $\langle r^2 \rangle_0 = \langle x^2 \rangle_0 + \langle y^2 \rangle_0 + \langle z^2 \rangle_0$

The macroscopic state of deformation may be assumed to be homogeneous: $\lambda_x=L_x/L_{x0}$; $\lambda_y=L_y/L_{y0}$; $\lambda_z=L_z/L_{z0}$.

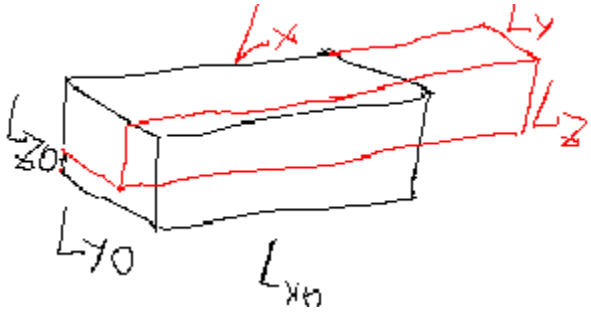

Assuming an isotropic network in the undeformed state:

$$\langle x^2\rangle_0 = \langle y^2\rangle_0 = \langle z^2\rangle_0 = \langle r^2\rangle_0 / 3$$

Two simple models

Affine Network Model

The junction points are assumed to be embedded in the network. As a result, components of each chain vector transform linearly with macroscopic deformation:

$$x = \lambda_x x_0; y = \lambda_y y_0; z = \lambda_z z_0 \qquad \langle x^2\rangle = \lambda_x^2\langle x^2\rangle_0; \langle y^2\rangle = \lambda_y^2\langle y^2\rangle_0; \langle z^2\rangle = \lambda_z^2\langle z^2\rangle_0$$

Substituting that in the eq.1

$$\Delta A_{el} = \frac{1}{2}\nu kT\left[\lambda_x^2+\lambda_y^2+\lambda_z^2-3\right]$$

More rigorous statistical mechanical analysis results in additional term

$$\Delta A_{el} = \frac{1}{2}\nu kT\left[\lambda_x^2+\lambda_y^2+\lambda_z^2-3\right]-\mu kT\ln\left(\frac{V}{V_0}\right)$$

This logarithmic term is usually negligible and =0 in incompressible limit.

The Phantom Network Model

Only a small number of junctions are assumed to be fixed at the surface and the remaining junctions fluctuate over time without being hindered by the presence of the neighboring chains. The instantaneous r-vector of each chain is a sum of a mean R and a fluctuation Δr: $r_i=R_i+\Delta r_i$. Then: $r_i^2=R_i^2+2R_i\Delta r_i+(\Delta r_i)^2$. $R_i\Delta r_i=0$ and after averaging:

$$\left\langle r^2\right\rangle=\left\langle R^2\right\rangle+\left\langle(\Delta r)^2\right\rangle=\left\langle X^2\right\rangle+\left\langle Y^2\right\rangle+\left\langle Z^2\right\rangle+\left\langle(\Delta x)^2\right\rangle+\left\langle(\Delta y)^2\right\rangle+\left\langle(\Delta z)^2\right\rangle$$

Theory relates equilibrium values:

$$\left\langle R^2\right\rangle_0=\left(1-\frac{2}{\phi}\right)\left\langle r^2\right\rangle_0;\left\langle(\Delta r)^2\right\rangle_0=\frac{2}{\phi}\left\langle r^2\right\rangle_0$$

Theory assumes that the components of R of each chain transforms affinely with macroscopic deformation, while Δr is not affected:

$$\left\langle X^2\right\rangle=\lambda_x^2\left\langle X^2\right\rangle_0;\left\langle Y^2\right\rangle=\lambda_y^2\left\langle Y^2\right\rangle_0;\left\langle Z^2\right\rangle=\lambda_z^2\left\langle Z^2\right\rangle_0;\left\langle(\Delta x)^2\right\rangle=\left\langle(\Delta x)^2\right\rangle_0;\left\langle(\Delta y)^2\right\rangle=\left\langle(\Delta y)^2\right\rangle_0;\left\langle(\Delta z)^2\right\rangle=\left\langle(\Delta z)^2\right\rangle_0;$$

As a result:

$$\left\langle r^2\right\rangle=\left[\left(1-\frac{2}{\phi}\right)\frac{\lambda_x^2+\lambda_y^2+\lambda_z^2}{3}+\frac{2}{\phi}\right]\left\langle r^2\right\rangle_0$$

and

$$\Delta A_{el}=\frac{1}{2}\xi kT\left(\lambda_x^2+\lambda_y^2+\lambda_z^2-3\right)$$

Thus both models predict:

$$\Delta A_{el}=FkT\left(\lambda_x^2+\lambda_y^2+\lambda_z^2-3\right)$$

$F=\nu/2$ for the affine network model and $F=\xi/2$ for the phantom network model. Because $\xi\approx(1-2/\phi)\nu$, the difference for network with $\phi=4$ is the factor 2!! $\xi<\nu$ and the phantom network model gives lower predictions than the affine network model

Let's consider simple elongation λ_x. For incompressible system $\lambda_x\lambda_y\lambda_z=1$, and $\lambda_z=\lambda_y=\lambda_x^{-1/2}$. Then

$$\Delta A_{el} = FkT\left(\lambda^2+\frac{2}{\lambda}-3\right);\ f=\frac{\partial \Delta A_{el}}{\partial \lambda}=2FkT\left(\lambda-\frac{1}{\lambda^2}\right) \qquad \textbf{(2)}$$

For small strain, $\lambda=1+e_{xx}$; $e_{xx}<<1$, we have Hookean law $f = 6FkTe_{xx} = Ee_{xx}$

The two models present two extremes. A real network is expected to exhibit properties that fall between those two extremes: junctions fluctuations do occur but they are limited. Limitations appear due to entanglements.

Stretching increases the space available to a chain along the direction of the stretch. The chain has more freedom to fluctuate. The same effect can appear during swelling because the separation between chains increases. As a result the modulus should decrease with stretching and swelling. This is supported by experimental results.

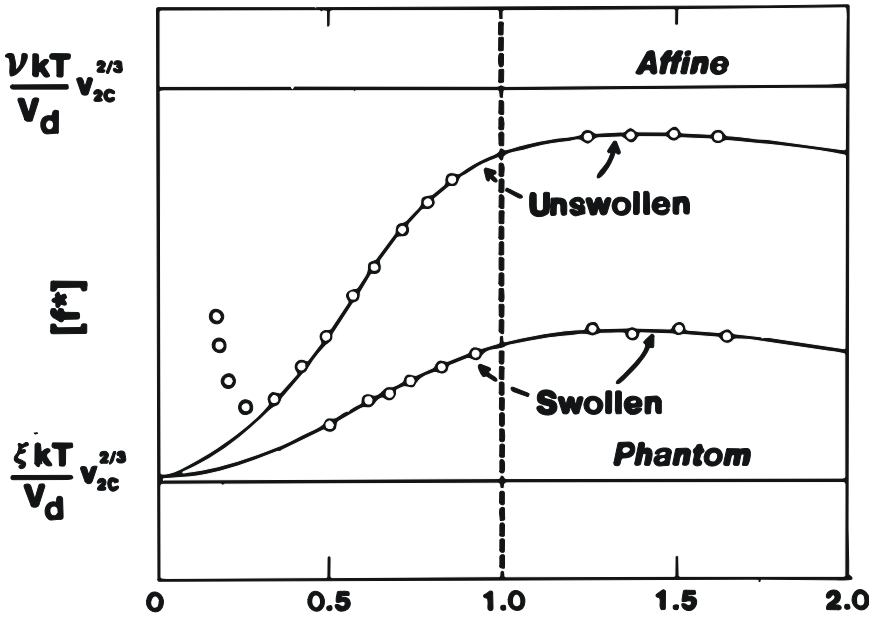

Constrained Junctions Model

The model assumes that the fluctuations of junctions are affected by interpenetration of chains.

A quantitative measure of the strength of the constraints is given by the ratio:

$$\kappa = \frac{\left\langle (\Delta R)^2 \right\rangle_{ph}}{\left\langle (\Delta s)^2 \right\rangle_0}$$

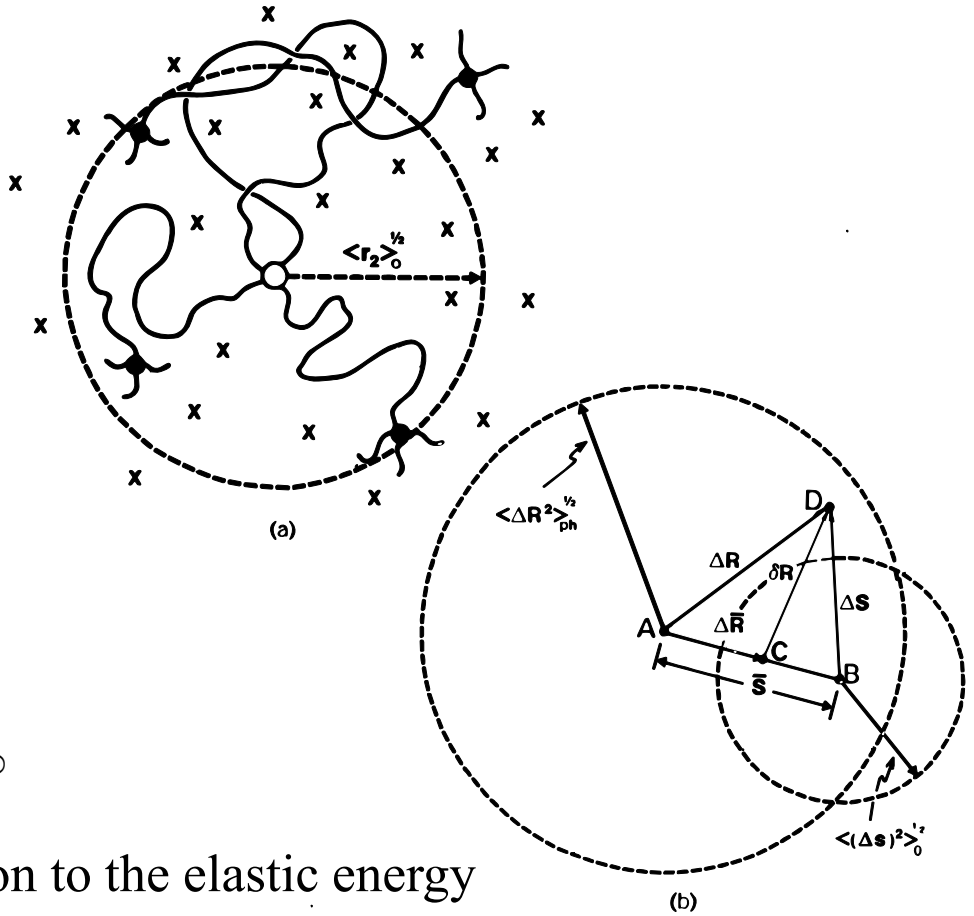

In the phantom limit: $\left\langle (\Delta s)^2 \right\rangle_0 \to \infty; \kappa \to 0$

In the affine limit: $\left\langle (\Delta s)^2 \right\rangle_0 \to 0; \kappa \to \infty$

Constraints provide additional contribution to the elastic energy

$$\Delta A_{el} = \Delta A_{ph} + \Delta A_c = \Delta A_{ph} + \frac{1}{2}\mu kT \sum_t \left[B_t + D_t - \ln(B_t + 1) - \ln(D_t + 1) \right], t = x, y, z$$

Where $B_t = \kappa^2 \dfrac{\lambda_t^2 - 1}{\left(\lambda_t^2 + \kappa\right)^2}$ and $D_t = \lambda_t^2 \kappa^{-1} B_t$

The constrained junction model describes the data reasonably well.

These three models focused on junctions. There are more complicated models that focus on chains and their constrains.

The affine network model and the phantom network model gives two limiting predictions for the rubber elasticity. They predict independence of the modulus on deformation and swelling. Experiment shows decrease of the modulus with swelling and extension.
This behavior is explained by the constrained junction model: Constraints decreases, $\langle(\Delta s)^2\rangle$ increases, and network becomes closer to the phantom network.

Rubber Reinforcement

As we considered above, rubber elasticity is entropic. There are only small energetic corrections introduced in more sophisticated theories.
As a result, the rubber modulus is usually weak (~10^5-10^6 Pa, usual materials ~10^9-10^{10} Pa). Increase in modulus is required for many applications.

One of the traditional ways of rubber reinforcements is addition of fillers. This way is widely used in practical applications. The two most important are:
- addition of *carbon black* to natural rubber and other carbon-based polymers;
- addition of *silica* to silicone rubbers.

The mechanism of the reinforcement on a molecular level is only poorly understood. One of the important mechanisms: chain may adsorb strongly onto the particle surfaces, increasing effectively degree of cross-linking.

Example of unfilled and filled PDMS networks at T=25C. The numbers correspond to the weight % of filler. The vertical dashed lines indicate the point of rupture. Significant increase in the modulus is achieved without lose of maximum extensibility.

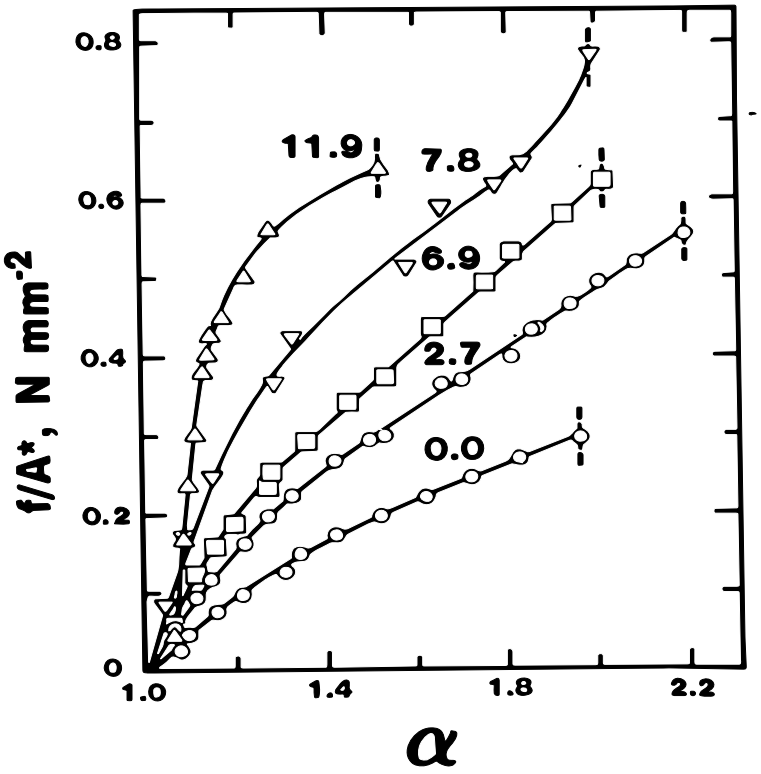

Detailed studies of structure and elasticity of silica-filled PDMS networks indicated a few important points:

- maximum reinforcement is obtained for particles with the size ~10-100 nm;
- a relatively narrow size distribution;
- very little of aggregation.

Networks with Multi-modal Chain Length Distribution

Previous considerations were based on an assumption of unimodal distribution of chain length. It was found that networks having multimodal chain-length distributions demonstrate significant improvements of properties. The new synthetic techniques that closely control the placements of cross-links allow preparation of a variety of model networks.

Example of bi-modal network

Typical plots of nominal stress against elongation for answollen bimodal PDMS networks. Long chains Mc~18000, and very short chains Mc~1100 (Δ), 660 (o) and 220 (•). Numbers show mol% of short chains. The area under each curve represents the rupture energy Er.

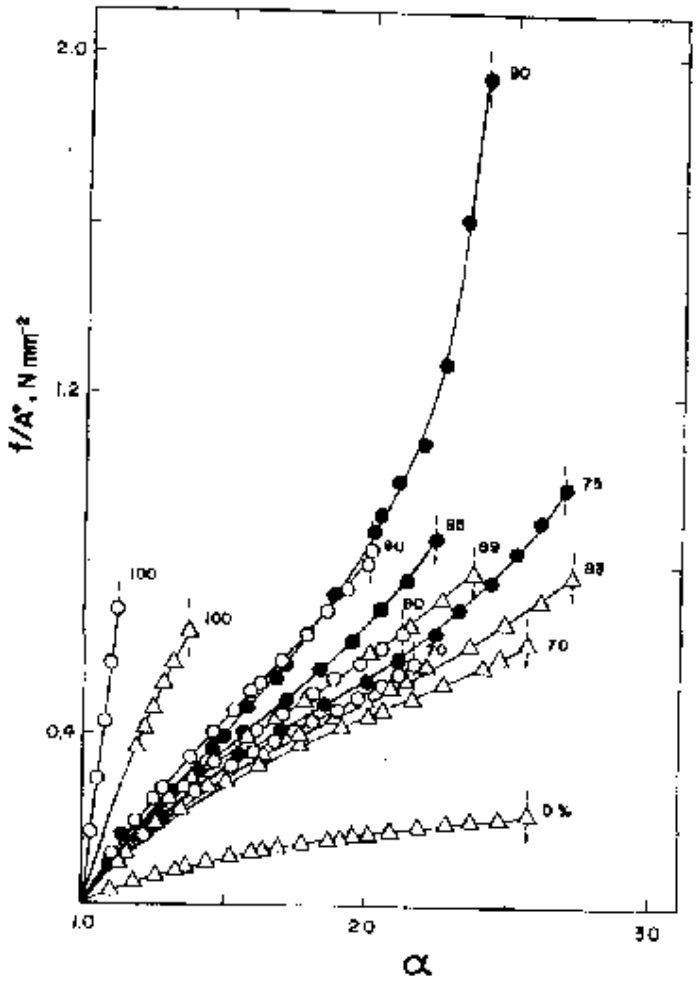

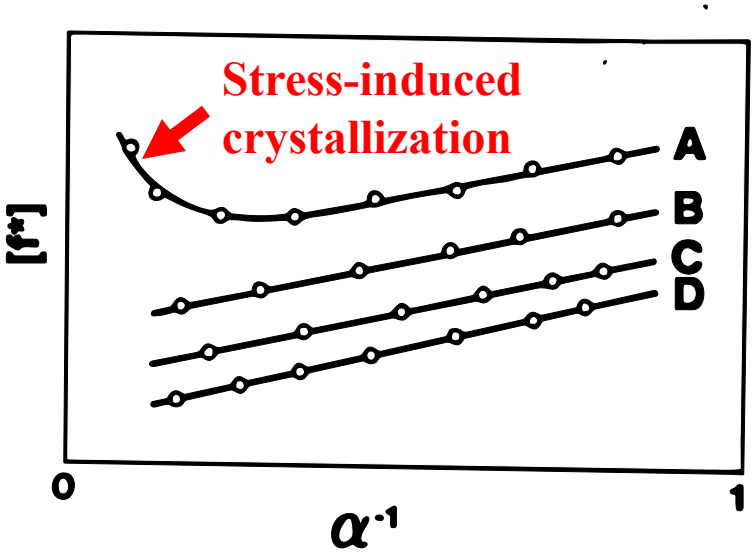

Unimodal networks:

A – crystallizable at low T;

B – the same network at higher T;

C – the same network, but swollen;

D – unimodal – non-crystallizable network.

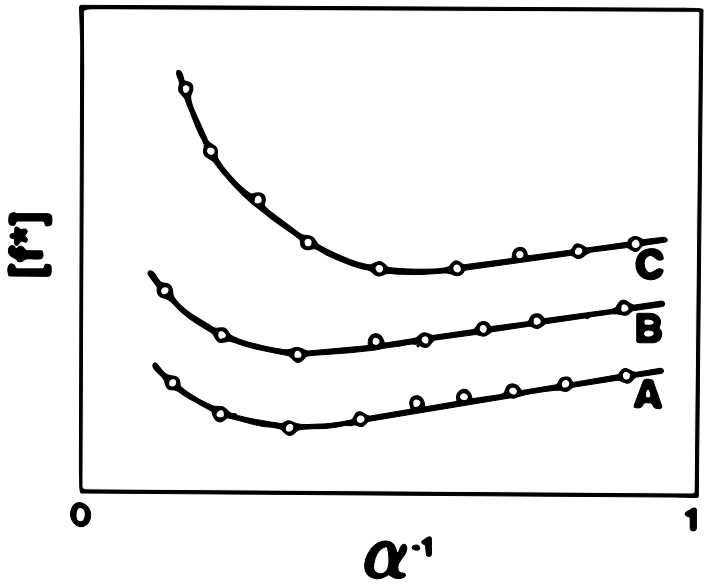

Non-crystallizable bimodal network:

C – low temperature;

B – higher temperature;

A – swollen network.

Reinforcement in bi-modal network is not due to crystallization. It is ascribed to limited extensibility of the short chains.

It is usually estimated that extension of the chain up to ~60-70% of chain length leads to appearance of significant energetic contribution (increase in modulus).

Looking ahead: Future of Polymer Science and Technology

We are moving from just consumer plastics and rubbers to more functional materials with polymers replacing many traditional materials (e.g. metals), and opening new horizons with 'smart' self-adopting, self-healing and stimuli-responsive materials:

- *Lightweight structural materials with strong mechanical properties*
- *Polymer electrolytes for batteries and fuel cells*
- *Membranes for molecular separation (e.g. CO_2 capture, water purification and desalination)*
- *Flexible and wearable electronics*
- *Materials for Additive Manufacturing (3D printing)*
- *Targeted drug delivery*
- *Tissue engineering (e.g. scaffolds, synthetic tissues …)*
- *Polymers from renewable sources, recyclable polymers*